Cell, Vol. 121, 859–872, June 17, 2005, Copyright ©2005 by Elsevier Inc. DOI 10.1016/j.cell.2005.03.036

WDR5 Associates with Histone H3 Methylated at K4 and Is Essential for H3 K4 Methylation and Vertebrate Development

Joanna Wysocka,[1,5] Tomek Swigut,[2,5] Thomas A. Milne,[1] Yali Dou,[3] Xin Zhang,[4] Alma L. Burlingame,[4] Robert G. Roeder,[3] Ali H. Brivanlou,[2] and C. David Allis[1,*]

[1]Laboratory of Chromatin Biology
[2]Laboratory of Molecular Vertebrate Embryology
[3]Laboratory of Biochemistry and Molecular Biology
The Rockefeller University
New York, New York 10021
[4]Mass Spectrometry Facility
University of California, San Francisco
San Francisco, California 94143

Summary

Histone H3 lysine 4 (K4) methylation has been linked to the transcriptional activation in a variety of eukaryotic species. Here we show that a common component of MLL1, MLL2, and hSet1 H3 K4 methyltransferase complexes, the WD40-repeat protein WDR5, directly associates with histone H3 di- and trimethylated at K4 and with H3-K4-dimethylated nucleosomes. WDR5 is required for binding of the methyltransferase complex to the K4-dimethylated H3 tail as well as for global H3 K4 trimethylation and *HOX* gene activation in human cells. WDR5 is essential for vertebrate development, in that WDR5-depleted *X. laevis* tadpoles exhibit a variety of developmental defects and abnormal spatial *Hox* gene expression. Our results are the first demonstration that a WD40-repeat protein acts as a module for recognition of a specific histone modification and suggest a mechanism for reading and writing an epigenetic mark for gene activation.

Introduction

Lysine methylation of histones is recognized as an important epigenetic indexing system demarcating transcriptionally active and inactive chromatin domains in eukaryotic genomes. For example, methylation of lysine 4 (K4) of histone H3 has been linked to transcriptional activation in a variety of eukaryotes (for review, see Sims et al. [2003]). To add to the complexity of epigenetic regulation, lysine residues can be mono-, di-, or trimethylated in vivo, and distinct methylation states are associated with different transcriptional outcomes. In particular, trimethylation of H3 K4 is strongly and preferentially associated with promoter and transcribed regions of active genes (Santos-Rosa et al., 2002; Schneider et al., 2004).

The first H3 K4 methyltransferase to be identified was the *S. cerevisiae* Set1 complex, whose catalytic subunit, the SET domain protein Set1, is homologous to the *Drosophila* trithorax protein and to a family of related human proteins, hSet1, MLL1, and MLL2, all of which are capable of methylating H3 at K4 (Roguev et al., 2001; Miller et al., 2001; Nagy et al., 2002; Milne et al., 2002; Nakamura et al., 2002; Wysocka et al., 2003; Hughes et al., 2004; Yokoyama et al., 2004). Human Set1-like enzymes are present in multiprotein complexes that appear to be structurally and functionally similar to the yeast Set1 complex (Wysocka et al., 2003; Goo et al., 2003; Hughes et al., 2004; Yokoyama et al., 2004). In humans, the MLL1 complex is recruited to promoters of homeobox (*Hox*) genes to maintain their activation state (Milne et al., 2002). In keeping with a transcriptional maintenance function(s), the activation state of *Hox* genes is epigenetically inherited through numerous cell divisions (reviewed in Francis and Kingston [2001]). These data suggest that H3 K4 methylation, facilitated by trithorax-related proteins, has a role in establishing "cellular memory" of transcription.

While progress has been made in identifying enzymes responsible for adding methyl groups to H3 K4, little progress has been made in characterizing the molecular effectors responsible for specifically recognizing this modification and translating it into a biological readout. A paradigm, however, has already been established for histone H3 K9 and K27 methylation. Here, specific effectors, chromodomain-containing proteins HP1 and Polycomb, associate with histone H3 methylated at K9 and K27, respectively, leading to changes in DNA template accessibility and higher-order changes in chromatin structure (Sims et al., 2003). Proteins that directly associate with H3 K4 methyl remain elusive, although a chromodomain protein Chd1 has been reported to bind to H3 methylated at K4 in yeast (Pray-Grant et al., 2005).

Using a biochemical approach to identify proteins that specifically recognize histone H3 methylated at K4, we identified WDR5, a highly conserved WD40-repeat protein, as a major methyl K4-associated protein in human cells and investigated its function in gene expression regulation and vertebrate development.

Results

WDR5 Is a Major H3-K4-Methyl-Associated Protein and a Common Component of Mammalian H3 K4 Methyltransferase Complexes

To identify proteins that bind to methylated H3 K4, we turned to an unbiased pull-down assay using biotinylated H3 peptide immobilized on avidin beads. Nuclear extracts from 293 cells were incubated with H3 peptides (aa 1–20 peptides; either unmodified or dimethylated at K4). Bound polypeptides were then eluted from the resin, resolved by SDS PAGE, and visualized by silver staining (Figure 1A). This analysis consistently revealed the presence of a single ~40 kDa band that was specifically enriched in the H3-K4-dimethylated peptide purification (see arrow in Figure 1A). The identity of this polypeptide was determined by mass spectrometry

*Correspondence: alliscd@rockefeller.edu
[5]These authors contributed equally to this work.

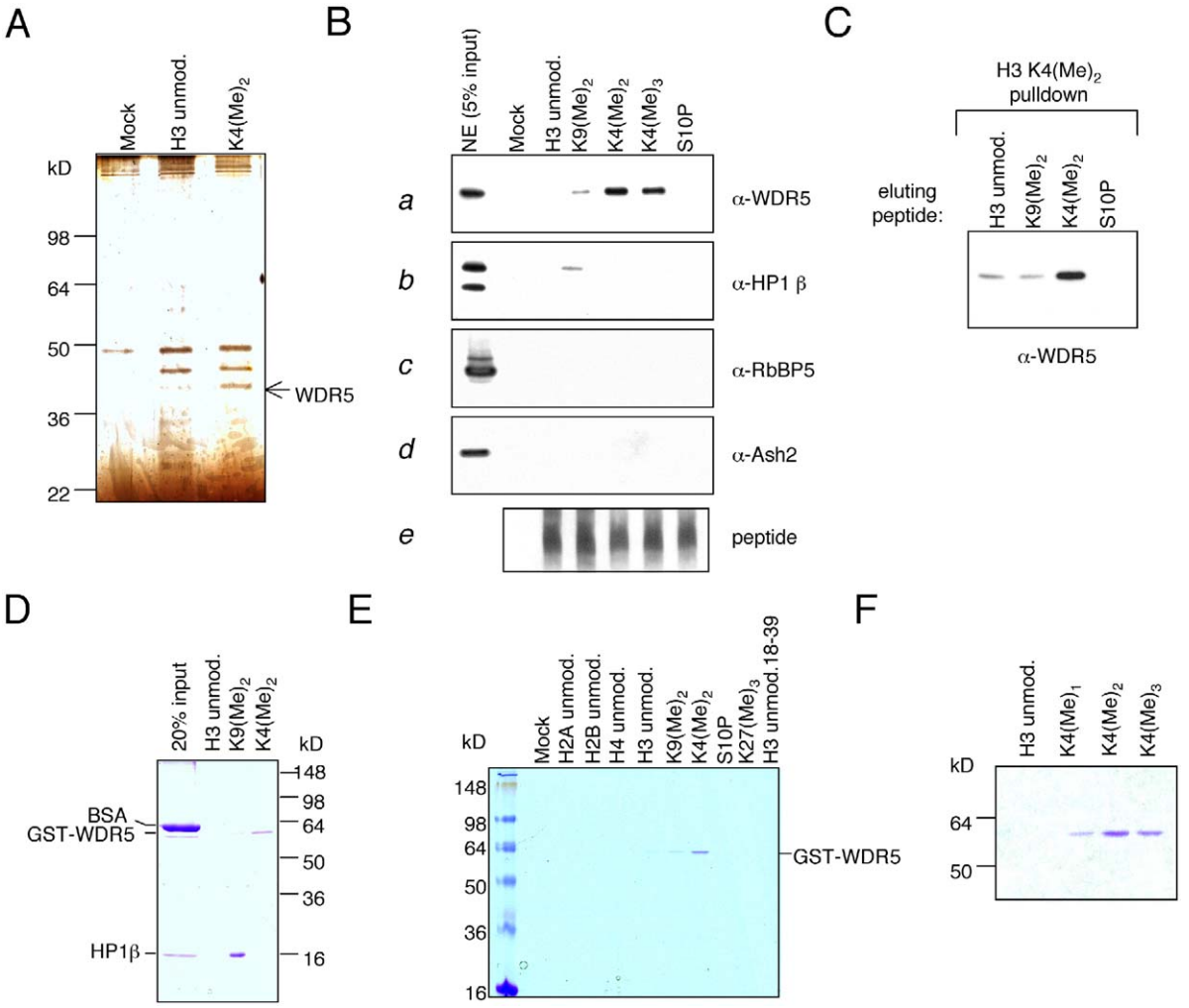

Figure 1. WDR5 Is a Major H3-K4-Methyl-Associated Protein

(A) Peptide pull-down assays were performed using 293 cell nuclear extracts and H3 peptides, either unmodified or dimethylated at K4. Polypeptides were resolved by SDS PAGE and visualized by silver staining. A polypeptide specifically enriched in the H3 K4$(Me)_2$ pull-down was analyzed by mass spectrometry and identified as WD40-repeat protein WDR5 (see arrow). Molecular weight markers are indicated on the left.

(B) Peptide pull-down assays using 293 nuclear extracts and a series of unmodified or appropriately modified H3 peptides (indicated on top) were performed and analyzed by immunobloting with α-WDR5 (Ba), α-HP1β (Bb), α-RbBP5 (Bc), and α-Ash2 (Bd) antibodies. After elution, beads were boiled in Laemmli buffer and peptide load analyzed by the silver staining (Be).

(C) Peptide pull-down assay was performed using 293 cells nuclear extract and H3 K4$(Me)_2$ peptide. Beads were divided into four equal portions and bound proteins eluted by competition with indicated peptides. Eluates were analyzed by immunoblotting with α-WDR5.

(D) 20-fold excess of BSA was incubated with equimolar amounts of purified recombinant HP1β and GST-WDR5 (each at 1 μg), and this mixture was used as input for the pull-down assay with indicated peptides. Bound proteins were analyzed by SDS PAGE and Coomassie blue staining. The position of each polypeptide is indicated on the left.

(E) Recombinant purified GST-WDR5 was used as input for pulldown assay, with various unmodified and modified histone-tail peptides indicated on top. Results were analyzed by SDS PAGE and Coomassie blue staining.

(F) Peptide pull-down assay with recombinant GST-WDR5 and H3 peptides either unmodified or mono-, di-, or trimethylated at K4.

and found to be the 333 amino acid long WD40-repeat protein WDR5, a common component of multiple H3 K4 methyltransferase complexes. Thus, similar to HP1, which associates with methylated H3 K9 and binds to the H3 K9 methyltransferase SUV39H1 (Bannister et al., 2001; Lachner et al., 2001; Aagaard et al., 1999), WDR5 associates with methylated H3 K4 and is present in various H3 K4 methyltransferase complexes.

WDR5 but Not RbBP5 Associates with Methylated H3 K4

To confirm the specificity of the association of WDR5 with H3 tail methylated at K4, we performed peptide pull-down assays using 293 nuclear extracts and a series of unmodified or appropriately modified H3 peptides (Figure 1B). Results were then analyzed by immunobloting with α-WDR5 antibody, or as a positive con-

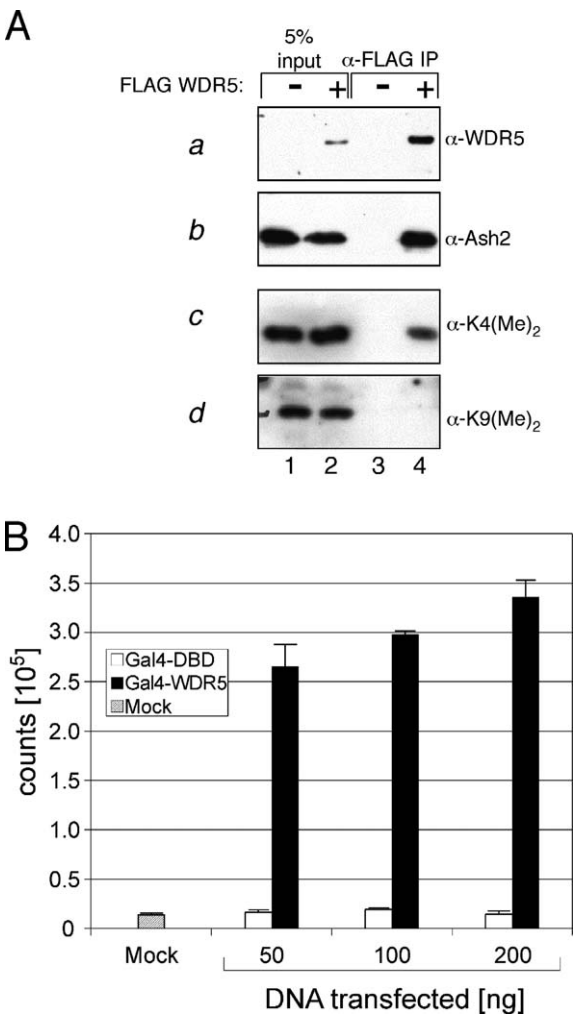

Figure 2. WDR5 Associates with Nucleosomes Methylated on H3 K4 and Activates Transcription

(A) Mononucleosomal fraction was purified from mock or Flag-WDR5 HeLa cell line and used for immunoprecipitation with α-Flag antibody followed by Flag peptide elution. Immunoprecipitates were analyzed by immunobloting with α-tagged WDR5 (α-FLAG; Aa), α-Ash2 (Ab), α-H3 K4(Me)$_2$ (Ac), and α-H3 K9(Me)$_2$ (Ad) antibodies. Five percent of input mononucleosomal fraction was used as a control.

(B) GAL4-WDR5 fusion activates transcription of a reporter gene. 293 cells stably expressing luciferase reporter under the control of GAL4 UAS were transfected in duplicates with indicated amounts of GAL4 DBD cDNA or GAL4-WDR5 cDNA, or mock transfected, and cell extracts were prepared. Relative luciferase activities (RLU) were measured for each sample and are shown as the average of three measurements of two independent transfections. Error bars represent standard deviation (SD).

trol, with α-HP1β antibody. As expected, HP1β associates specifically with the K9(Me)$_2$ H3 peptide (Figure 1Bb). In contrast, WDR5 preferentially associates with H3 that is either di- or trimethylated at K4 (Figure 1Ba). Although a weak association is also observed with H3 K9(Me)$_2$ peptide, significance of this binding is unclear, as we were unable to detect association of WDR5 with nucleosomes methylated at H3 K9 (see Figure 2A). WDR5 did not associate with H3 S10P peptide. Peptide competition experiments showed that H3 K4(Me)$_2$ peptide is more efficient in eluting the WDR5 protein prebound to K4-methylated H3 tail than either K9(Me)$_2$ or unmodified peptide, suggesting that K4-methylated H3 tail is the preferred binding substrate for WDR5 (see Figure 1C).

Despite the existence of multiple enzymatic subunits capable of methylating H3 K4, human H3 K4 methyltransferase complexes share three common components: two WD40-repeat proteins, WDR5 and RbBP5, and the trithorax group protein Ash2 (Wysocka et al., 2003; Goo et al., 2003; Hughes et al., 2004; Yokoyama et al., 2004). Thus, we sought to determine whether Ash2 and RbBP5 can bind to H3 methylated at K4. As shown in Figures 1Bc and 1Bd, neither Ash2 nor RbBP5 associated with any of the H3 peptides. These data, together with the fact that WDR5 is a major polypeptide enriched in the H3 K4(Me)$_2$ pull-down (Figure 1A), suggest that WDR5 specifically recognizes the H3 tail methylated at K4.

Association of WDR5 with H3 Methylated at K4 Is Direct and Specific

To further address whether interaction of WDR5 with K4-methylated H3 tail is direct, GST-WDR5 fusion protein was expressed in *E. coli* and purified to near homogeneity. To ensure specificity, the pull-down assay was performed with and excess of BSA (20 μg) and a 1:1 mixture of purified HP1β and GST-WDR5 (each at 1 μg). This mixture was then used as input for the pull-down assay with unmodified K9(Me)$_2$ and K4(Me)$_2$ peptides. As expected, HP1β was enriched in the K9(Me)$_2$ pull-down (Figure 1D). In contrast, WDR5 was enriched in the K4(Me)$_2$ pull-down, while BSA failed to bind to either peptide. Next, we tested binding of the purified GST-WDR5 to H2A, H2B, H4 (aa 1–20), and various unmodified and modified H3 peptides. As shown in Figure 1E, of the entire set of peptides tested, GST-WDR5 binding was specifically enriched in the H3 K4(Me)$_2$ peptide pull-down, indicating that association of WDR5 with H3 methylated at K4 is both direct and, within the context of the peptides used here, specific.

In order to investigate which K4 methylation state of H3 associates with WDR5, we tested binding of GST-WDR5 with a series of H3 peptides unmodified or mono-, di-, or trimethylated at K4. WDR5 preferentially associates with all forms of the H3-K4-methylated peptide as compared to unmodified peptide. Reproducibly, association with H3 K4(Me)$_2$ peptide is the most robust, while H3 K4(Me)$_1$ is the weakest (see Figure 1F).

WDR5 Associates with H3-K4-Methylated Mononucleosomes

To confirm the functional significance of WDR5 association with H3 peptides methylated at K4, we sought to address whether an in vivo association of WDR5 with H3-K4-methylated nucleosomes exists. Since the available WDR5 antibody fails to immunoprecipitate native protein, we took advantage of a HeLa cell line stably expressing Flag/HA epitope-tagged full-length WDR5. Total chromatin was isolated and solubilized with

micrococcal nuclease; fractions containing mononucleosomal DNA were then pooled and used for immunoprecipitation experiments with α-Flag antibody, followed by Flag peptide elution. To monitor specificity, chromatin from HeLa cells lacking ectopic WDR5 were used in parallel mock purifications. Immunoprecipitates were subsequently analyzed with antibodies against: (1) WDR5 (Figure 2Aa), to monitor immunoprecipitation efficiency; (2) Ash2 (Figure 2Ab), a known WDR5-associated protein, as a positive control; and (3) H3 methylated at K4 (Figure 2Ac) or K9 (Figure 2Ad). Results shown in Figures 2Ac and 2Ad demonstrate that WDR5 specifically coimmunoprecipitates with the H3-K4-methylated but not K9-methylated mononucleosomes (compare lanes 3 and 4 in Figures 2Ac and 2Ad). These data suggest that WDR5 binds to H3 tail methylated at K4 in vivo in the context of native chromatin.

WDR5 Is a Strong Transcriptional Activator

Di- and trimethylation of H3 K4 has been correlated with transcriptional activation in several organisms. Therefore, we hypothesized that WDR5, which preferentially recognizes di- and trimethylated H3 K4, may have transcriptional activation properties. To test this hypothesis, full-length human WDR5 cDNA, fused to the GAL4 DNA binding domain cDNA (GAL4-WDR5), was transfected into 293 cells stably expressing a luciferase reporter under the control of five tandem GAL4 UAS sites. Use of a stably integrated reporter in this assay ensured a dependency on the state of the chromatin template. Transfection of 50 ng of GAL4-WDR5 fusion cDNA resulted in 20-fold activation of the reporter, as compared to signals obtained from cells transfected with 50 ng of GAL4 DBD cDNA alone (Figure 2B). Comparison of GAL4-WDR5 with one of the strongest activators GAL4-VP16 revealed that activation by GAL4-WDR5 is ~10-fold weaker than GAL4-VP16-mediated activation (data not shown). Thus, when tethered to chromatin, WDR5 acts as a strong transcriptional activator.

Loss of WDR5 Affects Global H3 K4 Methylation Levels in Human Cells without Affecting Global Association of MLL1, MLL2, and Ash2 with Chromatin

One potential mechanism by which WDR5 activates transcription may be by facilitating methylation of H3 K4. To address whether WDR5 knockdown may have a global effect on the steady-state level of H3 K4 methylation, WDR5 protein was specifically eliminated by transfecting 293 cells with a pool of four WDR5 siRNAs. 293 cells transfected with the corresponding amounts of noncoding siRNAs served as a control. Whole-cell extracts were prepared 3 days after transfection and analyzed by immunoblotting with various antibodies.

WDR5 siRNA transfection resulted in the efficient knockdown of WDR5 protein (Figure 3Aa) but did not affect expression levels of other components of H3 K4 methyltransferases, Ash2, MLL1, and MLL2 (Figures 3Ab, 3Ac, and 3Ad). However, global levels of the K4 methylation were significantly reduced in WDR5 siRNA-transfected cells with a strong decrease of H3 K4 mono- (Figure 3Ae) and trimethylation (Figure 3Ag) and only a modest effect on dimethylation (Figure 3Af). Little or no effect was observed on H3 K9 and K27 trimethylation (Figures 3Ai and 3Aj) and unmodified histone H3 (Figure 3Ah); global histone levels were also not affected (Figure 3Ak). Similar results were obtained with extracts from cells transfected with each individual siRNA from the pool of four siRNAs (data not shown).

The global effect of WDR5 knockdown on H3 K4 methylation may be due to its effect on chromatin association of other proteins directly involved in H3 K4 methylation. To ask whether global chromatin association of components of human H3 K4 methyltransferases is affected by the loss of WDR5 protein, we took advantage of a small-scale biochemical fractionation scheme originally developed by Mendez and Stillman (Mendez and Stillman, 2000) and depicted in Figure 3B. Although each fraction has a distinct polypeptide composition, as expected, histones are recovered in the chromatin fraction P3 (Figure 3Cf, lanes 3 and 6). The distribution of WDR5, different H3 K4 methyltransferases, and several of their complex components were then examined by immunoblotting with specific antibodies (Figures 3Ca–3Ce).

As shown in Figure 3Ca, in cells transfected with control siRNA, a portion of WDR5 is associated with chromatin (lane 3), and a portion is recovered in S2 soluble fraction (lane 1). In contrast, transfection of cells with WDR5 siRNA pool resulted in loss of WDR5 from both soluble and chromatin fractions (lanes 4 and 6). Immunoblot analyses with α-Ash2, α-RbBP5, α-MLL1, and α-MLL2 antibodies (Figures 3Cb–3Ce) revealed that there is no effect of WDR5 knockdown on the global association of these proteins with chromatin (compare lanes 3 and 6 in all panels). Thus, the effect of WDR5 knockdown on H3 K4 methylation cannot be explained simply by the loss of methyltransferase association with chromatin.

WDR5 Is Required for Association of the Methyltransferase Complex with H3-K4-Dimethylated Substrate

To address the mechanism by which loss of WDR5 affects H3 K4 methylation without affecting association of H3 K4 methyltransferases with chromatin, we characterized binding of the H3 K4 methyltransferase complexes to either unmodified, K4 di-, or trimethylated H3 peptides. To this end, we took advantage of two HeLa cell lines stably expressing (1) Flag/HA epitope-tagged full-length WDR5 or (2) Flag/HA epitope-tagged full-length RbBP5 (Dou et al. [2005], this issue of *Cell*). Nuclear extracts were fractionated on P11 phosphocellulose. Fractions containing (1) both free WDR5 and WDR5 associated with hSet1 and MLL2 methyltransferase complexes or (2) both free RbBP5 and RbBP5-associated hSet1 and MLL2 methyltransferase complexes were subjected to anti-Flag immunoprecipitation followed by Flag peptide elution (depicted in Figure 4A). Purified material was then used as input for the peptide pull-down assays with unmodified or K4 di- or trimethylated H3 peptides. Immunoblot analysis reveals that Flag-WDR5 preferentially associates with di- and, to a lesser extent, trimethylated peptide, with only a minor association with the unmodified peptide (Figure 4Ba).

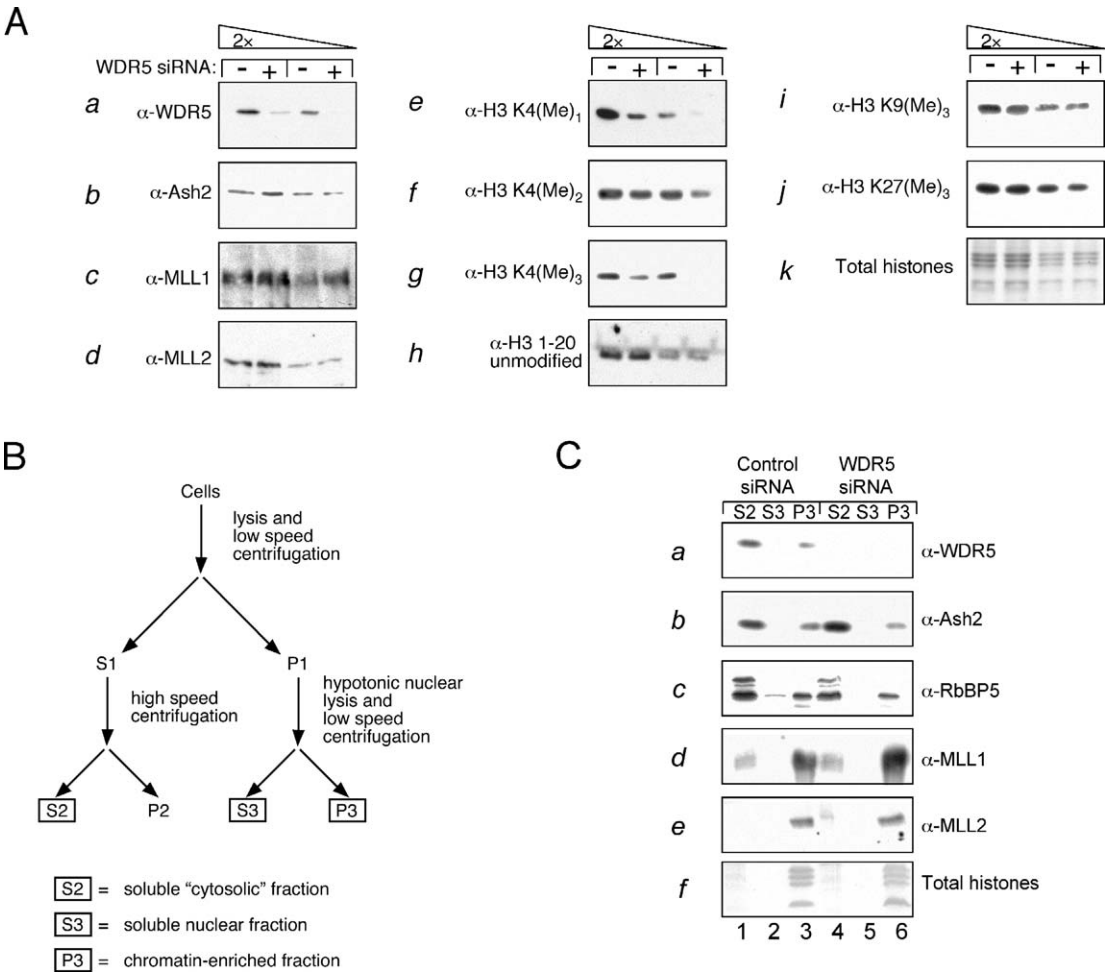

Figure 3. Loss of WDR5 Affects Global H3 K4 Methylation Levels but Not MLL1, MLL2, or Ash2 Chromatin Association

(A) Analysis of effects of WDR5 knockdown on histone H3 K4 methylation. 293 cells were transfected with control siRNAs or WDR5 siRNA pool and counted, and whole-cell extracts were prepared 3 days after transfection and probed by immunoblotting with α-WDR5 (Aa), α-Ash2 (Ab), α-MLL1 (Ac), α-MLL2 (Ad), H3 K4$(Me)_{1-3}$ (Ae–Ag), α-H3 1–20 unmodified (Ah), α-H3 K9$(Me)_3$ (Ai), α-H3 K27$(Me)_3$ (Aj) antibodies or stained with Coomassie blue for total histones to ensure equal loading (Ak). Two-fold dilution of each extract was used in order to control for the dynamics of the antibody response.

(B) Biochemical fractionation scheme. Final fractions used for analysis—soluble "cytosolic" (S2), soluble nuclear (S3), and chromatin-enriched (P3)—are boxed. The cytosolic fraction S2 also contains soluble nuclear components owing to permeabilization of the nuclear membrane during cell lysis with nonionic detergent.

(C) Loss of WDR5 has no effect on global chromatin association of MLL1, MLL2, Ash2, and RbBP5. 293 cells were transfected with control siRNAs or WDR5 siRNA pool and subjected to biochemical fractionation. Fractions S2, S3, and P3 were probed by immunoblotting with α-WDR5 (Ca), α-Ash2 (Cb), α-RbBP5 (Cc), α-MLL1 (Cd), and α-MLL2 (Ce) antibodies and stained with Coomassie blue for analysis of total histones distribution (Cf). All fractions were resuspended in equal final volumes and thus represent the cellular distribution of the analyzed proteins.

These data are consistent with the binding specificity of recombinant WDR5 (Figure 1F). In contrast, other components of the H3 K4 methyltransferase complex—RbBP5, Ash2, and MLL2—bind equally well to the unmodified and dimethylated peptides and poorly to the trimethylated peptide (Figures 4Bb–4Bd). As all of the proteins present in the input are associated with Flag-WDR5, these results suggest that free Flag-WDR5, present in excess, preferentially associates with K4-dimethylated H3, whereas H3 K4 methyltransferase complexes associate both with unmodified and K4-dimethylated H3. Consistent with these observations, immunoblot analysis of the pull-down with Flag-RbBP5 demonstrates that all of the tested complex components, including WDR5, bind both to unmodified and dimethylated peptides (Figure 4C). Furthermore, only a small fraction of Flag-RbBP5 is recovered in the pull-down, as compared to Flag-WDR5 (compare Figures 4Ca and 4Ba), suggesting that RbBP5 is unlikely to bind histone H3 tail on its own and that observed association reflects specificity of the methyltransferase complex. Interestingly, in the experiments presented in Figure 1B, we failed to detect binding of RbBP5 and Ash2 to any of the H3 peptides or binding of WDR5 to the unmodified peptide, which is likely due to the fact that proteins bound in the complex were below sensitivity

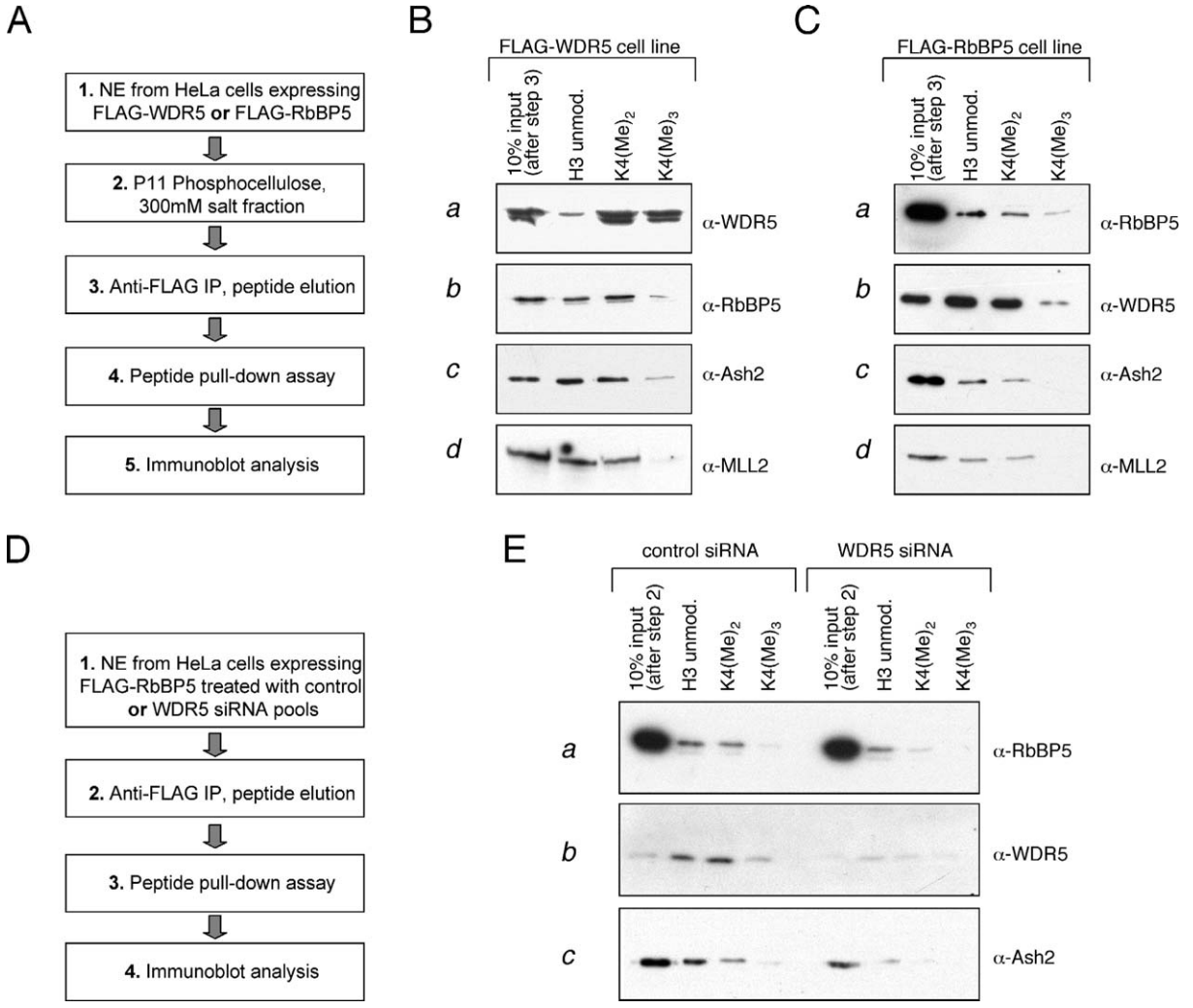

Figure 4. WDR5 Is Important for Binding of the H3 K4 Methyltransferase Complex to Dimethylated H3 K4

(A) Schematic of the experimental design.

(B) Flag-WDR5 and its associated proteins were purified from stable Flag-WDR5 HeLa cell line as depicted in (A) and used as input for the peptide pull-down assay with indicated peptides. Results were analyzed by immunoblotting with α-WDR5 (Ba), α-RbBP5 (Bb), α-Ash2 (Bc), and α-MLL2 (Bd) antibodies.

(C) Flag-RbBP5 and its associated proteins were purified from stable Flag-RbBP5 HeLa cell line as depicted in (A) and used as input for the peptide pull-down assay with indicated peptides. Results were analyzed by immunoblotting with α-RbBP5 (Ca), α-WDR5 (Cb), α-Ash2 (Cc), and α-MLL2 (Cd) antibodies.

(D) Schematic of the experimental design for data presented in (E).

(E) Flag-RbBP5 cells were transfected with control siRNAs or WDR5 siRNA pool, and nuclear extracts were prepared 3 days after transfection. Flag-RbBP5 and its associated proteins were purified and used for peptide pull-down assay as depicted in (D). Results were analyzed by immunobloting with α-RbBP5 (Ea), α-WDR5 (Eb), and α-Ash2 (Ec) antibodies.

of our assay. This also indicates that majority of the endogenous WDR5 is present in the nuclear extract in its free form, either because the majority of complexes fall apart during the nuclear extract preparation or due to excess of WDR5 naturally present in the nucleus.

Results presented in Figure 4B and C suggest that WDR5-containing H3 K4 methyltransferase complexes have dual binding specificity toward the H3 tail, i.e., they bind to both unmodified and K4-dimethylated H3 tail. We hypothesized that WDR5 provides specificity toward the dimethylated tail, whereas another component is responsible for binding of the complex to the unmodified histone H3 tail. To test this hypothesis, we purified Flag-RbBP5 and associated proteins from the Flag/HA-RbBP5 cells treated with control siRNA or WDR5 siRNA, as schematically depicted in Figure 4D. As shown in Figure 4E, WDR5 knockdown resulted in loss of binding of RbBP5 and Ash2 to dimethylated but not unmodified peptide. These findings are consistent with our observations that loss of WDR5 does not affect chromatin association of methyltransferase complex components and strongly suggests that WDR5 endows the MLL methyltransferase complex with an ability to bind to dimethylated substrates. We also noted de-

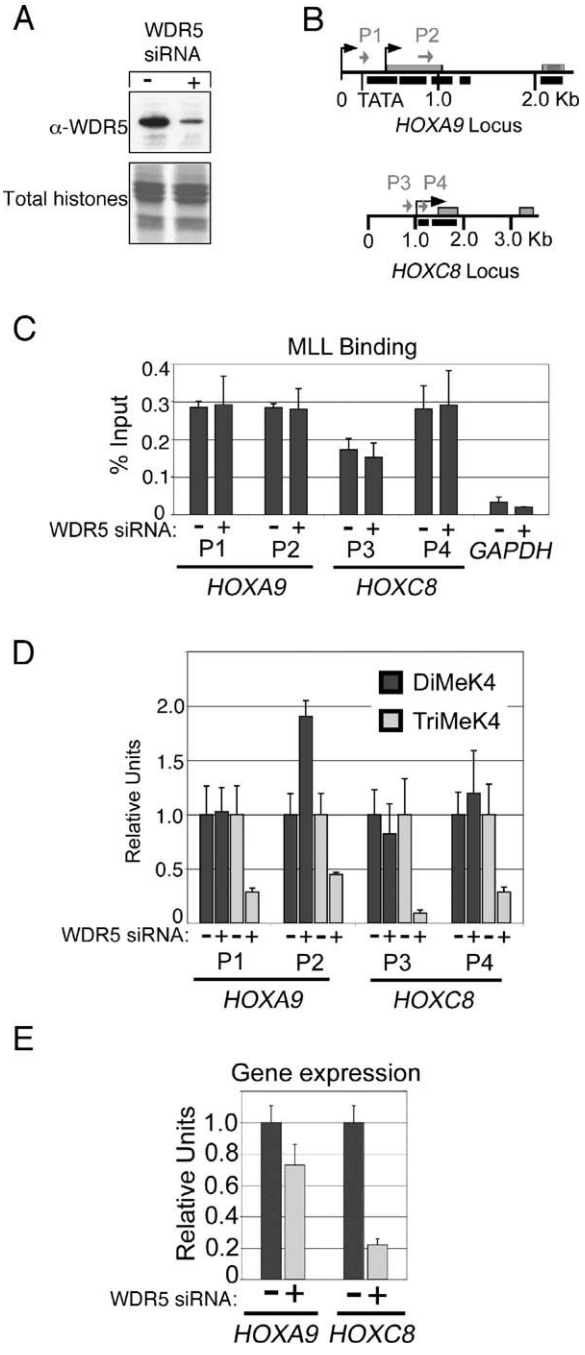

Figure 5. Loss of WDR5 Protein Results in a Decrease of Histone H3 Lysine 4 Trimethylation but Not Dimethylation at *HOX* Genes

(A) Treatment of 293 cells with WDR5 siRNA (+) results in a decrease of WDR5 protein levels compared to control (–) cells transfected with noncoding siRNA.

(B) Schematic of the *HOXA9* and *HOXC8* loci. Gray arrows mark the positions of Taqman primer/probe sets (P1–P4) used to quantify ChIP experiments. Gray boxes represent exons, black arrows are transcription start sites, and black boxes represent CpG rich regions. A putative TATA box at the *HOXA9* locus identified by Nakamura et al. (2002) as a site of MLL binding is also shown. Distances are in kilobases.

(C) Binding of MLL to the promoter and coding regions of *HOXA9* and *HOXC8* is not altered by a reduction of WDR5 protein. Primer/probe sets are as shown in (B). Signal was quantified relative to input chromatin as described in Experimental Procedures. Background signal was determined in *Mll*$^{-/-}$ cells to be lower than 0.05% (data not shown). Binding at the *GAPDH* locus is shown as a control and is below background levels. Error bars represent SD based on three independent experiments.

(D) Histone H3 K4$(Me)_3$ (light gray bars) but not K4$(Me)_2$ (dark gray bars) is reduced by WDR5 siRNA treatment (+) compared to cells treated with a control siRNA (–). ChIP experiments were quantified as in (C), but signals from WDR5 siRNA-treated cells (+) were standardized relative to signal from control cells (–), which were set to 1.0. Primer/probe sets are as shown in (B). Error bars represent SD based on three independent experiments.

(E) Treatment of 293 cells with WDR5 siRNA (+) reduces *HOXA9* and *HOXC8* gene expression compared to cells treated with a control siRNA (–). Gene expression was quantified using *βACTIN* as an internal standard. Expression of *HOX* genes in WDR5 siRNA treated cells (+) is standardized relative to expression in control cells (–). Error bars represent SD based on three independent experiments.

creased association of Ash2 with RbBP5 in WDR5-depleted cells, suggesting that WDR5 stabilizes Ash2 association with the complex (Figure 4Ec).

Taken together, our data suggest a model in which WDR5 does not play a role in the recruitment of its associated methyltranferase complex to localized region of chromatin and in the initiation of methylation but instead is important for di- to trimethyl lysine convertion. We sought to test this hypothesis at the localized region of chromatin, known to be regulated by the WDR5-associated methyltransferase.

WDR5 Knockdown Does Not Affect MLL1 Recruitment to the *HOXA9* and *HOXC8* Loci

To determine whether loss of WDR5 affects the recruitment of its associated methyltransferase to a localized region of chromatin, we examined if WDR5 knockdown has any effect on the recruitment of one of its associated methyltransferases, MLL1, to two of its known targets, the *HOXA9* and *HOXC8* genes. To this end, 293 cells were transfected with a pool of WDR5 siRNAs or with control noncoding siRNA. Samples were normalized by cell counting and used for whole-cell extract and total RNA preparations; knockdown efficiency was confirmed by immunoblotting (Figure 5A). Remaining cells were used for a chromatin immunoprecipitation assay (ChIP) with α-MLL1 antibody. To determine whether association of MLL1 with either the *HOXA9* or *HOXC8* locus is affected by the WDR5 knockdown, the immunoprecipitated DNA was quantified by real-time PCR using probes to the *HOXA9* promoter and gene coding region and *HOXC8* promoter and 5′ leader sequence (see Figure 5B). As a negative control, a probe to the *GAPDH* control locus was used. As shown in Figure 5C, reduction of WDR5 levels did not have any measurable effect on the association of MLL with the *HOXA9* and *HOXC8* loci, suggesting that WDR5 does not act through the recruitment of this K4 methyltransferase to its target loci. As expected, no MLL binding was observed at the *GAPDH* locus. Consistent with our previous results, this suggests that WDR5 does not directly recruit methyltransferases such as MLL1 to target loci.

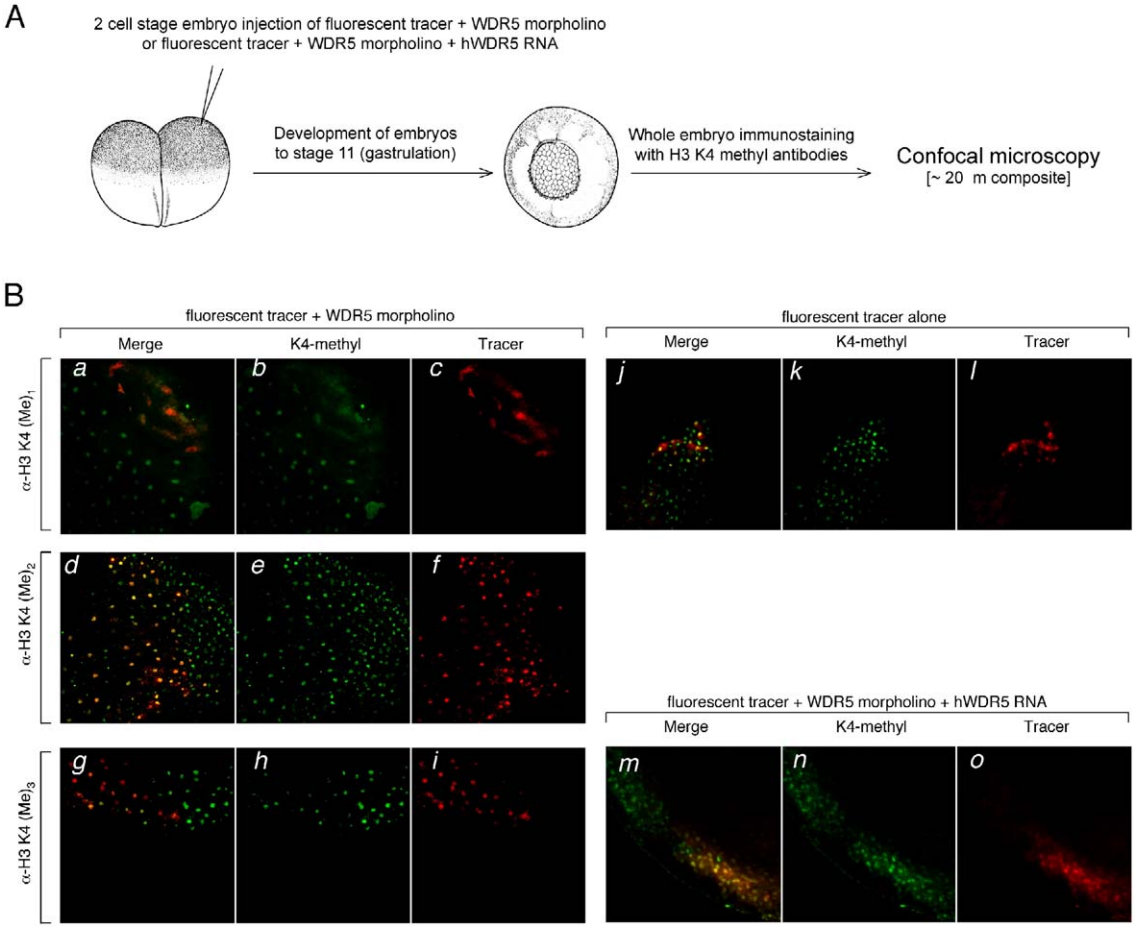

Figure 6. WDR5 Knockdown in *X. laevis* Embryos Results in Loss of Mono- and Trimethylation of H3 K4

(A) Schematic of experimental design.

(B) Two-cell stage *X. laevis* embryos were coinjected with xWDR5 morpholino and Alexa-647-dextran fluorescent lineage tracer (Ba–Bi) or with xWDR5 morpholino, Alexa-647-dextran tracer and synthetic mRNA encoding human GST-WDR5 (Bm–Bo), or as negative control, with Alexa-647-dextran alone (Bj–Bl). Embryos were allowed to develop to stage 11, fixed, immunostained with H3 K4 methyl antibodies (green), followed by Alexa-555-conjugated anti-rabbit secondary antibodies (red), and analyzed by confocal microscopy. Panels show a combination of 20 focal planes corresponding to approximately 20 μm section stacks of the embryo.

WDR5 Knockdown Leads to the Decrease in the H3 K4 Trimethylation but Not H3 K4 Dimethylation over the *HOXA9* and *HOXC8* Loci

Next, we asked whether WDR5 knockdown affects the status of K4 methylation at the *HOXA9* and *HOXC8* genes, known targets of MLL-mediated activation. ChIP assays were performed with antibodies against H3 either di- or trimethylated at K4. Immunoprecipitated DNA was then subjected to quantitative real-time PCR using probes to the *HOXA9* and *HOXC8* genes (Figure 5B). As shown in Figure 5D, WDR5 knockdown did not affect H3 K4 dimethylation over the promoter regions of *HOXA9* and *HOXC8* and 5′ leader sequence of HOXC8. Interestingly, we reproducibly observed an increase of K4 dimethylation over the coding region of *HOXA9* upon loss of WDR5. In contrast, WDR5 knockdown resulted in a significant and reproducible decrease in H3 K4 trimethylation over *HOXA9* and *HOXC8* genes (Figure 5D). Similar results were obtained using two α-H3 K4 trimethyl antibodies and four independent knockdown/ChIP experiments (data not shown). Our results demonstrate that WDR5 contributes to the majority of K4 trimethylation at the *HOX* loci and are consistent with a model wherein WDR5 is important for the di- to trimethyl conversion by the H3 K4 methyltransferase complex.

WDR5 Is Important for Maintenance of *HOX* Gene Expression

To test whether WDR5 knockdown has an effect on the expression of *HOXA9* and *HOXC8* genes, a portion of the same set of samples used for the above ChIP experiments was used for the total RNA preparation and quantitative real-time RT-PCR analysis. As shown in Figure 5E, knockdown of WDR5 expression resulted in 5-fold downregulation of *HOXC8* mRNA levels and a minor but reproducible downregulation of *HOXA9* mRNA levels, as compared to cells transfected with control siRNAs. These results also correlate with stronger effect of WDR5 loss on K4 trimethylation on

the *HOXC8* locus, compared to the *HOXA9* locus, which may reflect differences in the dynamic transcriptional regulation of the two genes. Whichever the case, these results demonstrate that WDR5 function is important for *HOX* gene regulation in human cells.

WDR5 Is Essential for H3 K4 Methylation in *X. laevis*

Our data suggest that WDR5 affects global H3 K4 methylation levels and expression of *HOX* genes in human cells. It was of interest to know if these observations could be reproduced on an organismal level and, if so, what the effect of perturbations in K4 methylation on the development of a vertebrate organism would be. Evolutionary conservation of WDR5 is quite remarkable. With the exception of the N-terminal "tail," whose length and sequence is variable among different species, the part of the protein that encompasses the seven WD40 repeats has a very high degree of sequence identity among the metazoan species (see Figure S1 in the Supplemental Data available with this article online). Given evolutionary conservation of WDR5, we sought to address the above questions using *X. laevis* as a developmental system and morpholino antisense technology to block translation of *X. laevis* xWDR5 mRNAs.

A morpholino oligonucleotide overlapping with the ATG codon of *X. laevis* WDR5 (xWDR5 morpholino) was designed and injected into the marginal zone of one blastomere of a two-cell stage *X. laevis* embryo. To trace the progeny of injected blastomeres, injections also included a fluorescent lineage tracer (red-stained cells). As depicted in Figure 6A, embryos were then allowed to develop to midgastrula stage (stage 11), after which in situ immunostaining was performed with the α-H3 K4 methyl antibodies followed by confocal microscopy. The noninjected side of the embryo served as an internal control. Results of these experiments are shown in Figure 6B. A striking inverse correlation was observed between intensity of staining with the α-H3 K4 mono- (Figures 6Ba–6Bc) and trimethyl (Figures 6Bg–6Bi) antibodies (green) and the presence of the fluorescent tracer (red), suggesting that xWDR5 knockdown results in a reduction of K4 mono- and trimethylation in *Xenopus* embryos. Consistent with the results obtained in mammalian cells, xWDR5 morpholino injection did not have a significant effect on α-K4$(Me)_2$ staining (Figures 6Bd–6Bf); no reduction in H3 K4 methyl staining was observed in embryos injected with the fluorescent tracer alone (example shown in Figures 6Bj–6Bl). To control for the specificity of the observed effects, WDR5 morpholino was coinjected with the in vitro-transcribed GST-hWDR5 RNA. As shown in Figures 6Bm–6Bo, GST-hWDR5 RNA reverted the effect of the xWDR5 morpholino on K4 trimethylation, as cells containing fluorescent tracer stained for trimethylation with an intensity similar to that of cells that are tracer negative. Furthermore, xWDR5 morpholino injection into one-cell embryos results in a global loss of WDR5 protein and H3 K4 trimethylation (Figure 7B).

Knockdown of xWDR5 during *Xenopus* Development Leads to Somitic, Gut, and Hematopoetic Defects

To date, no WDR5 loss-of-function analysis has been done in any vertebrate organism, and the general role of K4 methylation in vertebrate development is poorly understood. Thus, the *X. laevis* model provides a unique opportunity to look at the effects of loss of WDR5 and, in consequence, a reduction of global K4 methylation levels on the development of a vertebrate. To this end, one-cell stage *X. laevis* embryos were injected with WDR5 morpholino, and the injected embryos were allowed to develop to the feeding tadpole stages. To eliminate synthetic phenotypes resulting from different genetic backgrounds, the analysis was performed on embryos derived from eggs of multiple frogs (n = 6).

In general, tadpoles derived from xWDR5 morpholino-injected embryos were delayed in development by as much as four stages compared to the tadpoles derived from control-injected embryos. These embryos exhibited a variety of developmental defects: mesodermal axial defects resulting in shortened and twisted tadpoles as well as gut patterning defects, resulting in lack of gut coiling and ventral lesions (see Figures 7Aa–7Ac). These phenotypes were highly penetrant and were effectively rescued by the coinjection of GST-hWDR5 mRNA along with xWDR5 morpholino (Figures 7Ad and 7C). Injection of the GST-hWDR5 mRNA alone had no significant effect on development (Figures 7Ae and 7C), and phenotype penetrance and severity were dependent on xWDR5 morpholino dose (data not shown). Taken together, these observation indicate that observed phenotypes are specific to the WDR5 protein level knockdown and cannot be attributed to some unspecific effect of the morpholino oligonucleotide injection. Immunoblot analysis of extracts prepared from single embryos that were control injected, xWDR5 morpholino injected, or coinjected with xWDR5 morpholino and GST-hWDR5 mRNA revealed that morpholino injection results in global loss of xWDR5 protein and H3 K4 trimethylation (compare Figures 7Ba–7Bc, lanes 1 and 2). Coinjection of GST-hWDR5 mRNA resulted in expression of GST-hWDR5 fusion protein and in the rescue of H3 K4 trimethylation (Figure 7B, see lane 3 in all panels).

Phenotypic analyses were also performed with two- to four-cell stage embryos injected with xWDR5 morpholino into one blastomere (either dorsal or ventral). Tadpoles derived from single blastomere-injected embryos exhibited somewhat milder phenotypes. In particular, ventral lesions where absent and axial defects limited to a lateral bend. As shown in Figure 7D, xWDR5 morpholino-injected tadpoles exhibited somitic defects on one side of the body, resulting in a distinctive bend (different from more random shortening and twisting that was observed for one-cell-stage-injected embryos) as well as delayed or absent gut (see Figure 7E for statistical analysis of the penetrance of phenotypes presented in Figure 7D). Many of the tadpoles also exhibited hematopoetic abnormalities consistent with ventral mesoderm defects: no blood, or blood missing from the heart, while forming extensive internal hemorrhages. These results indicate that WDR5 function, and presumably transcriptional profiles determined in part by K4 methylation, is essential for vertebrate development.

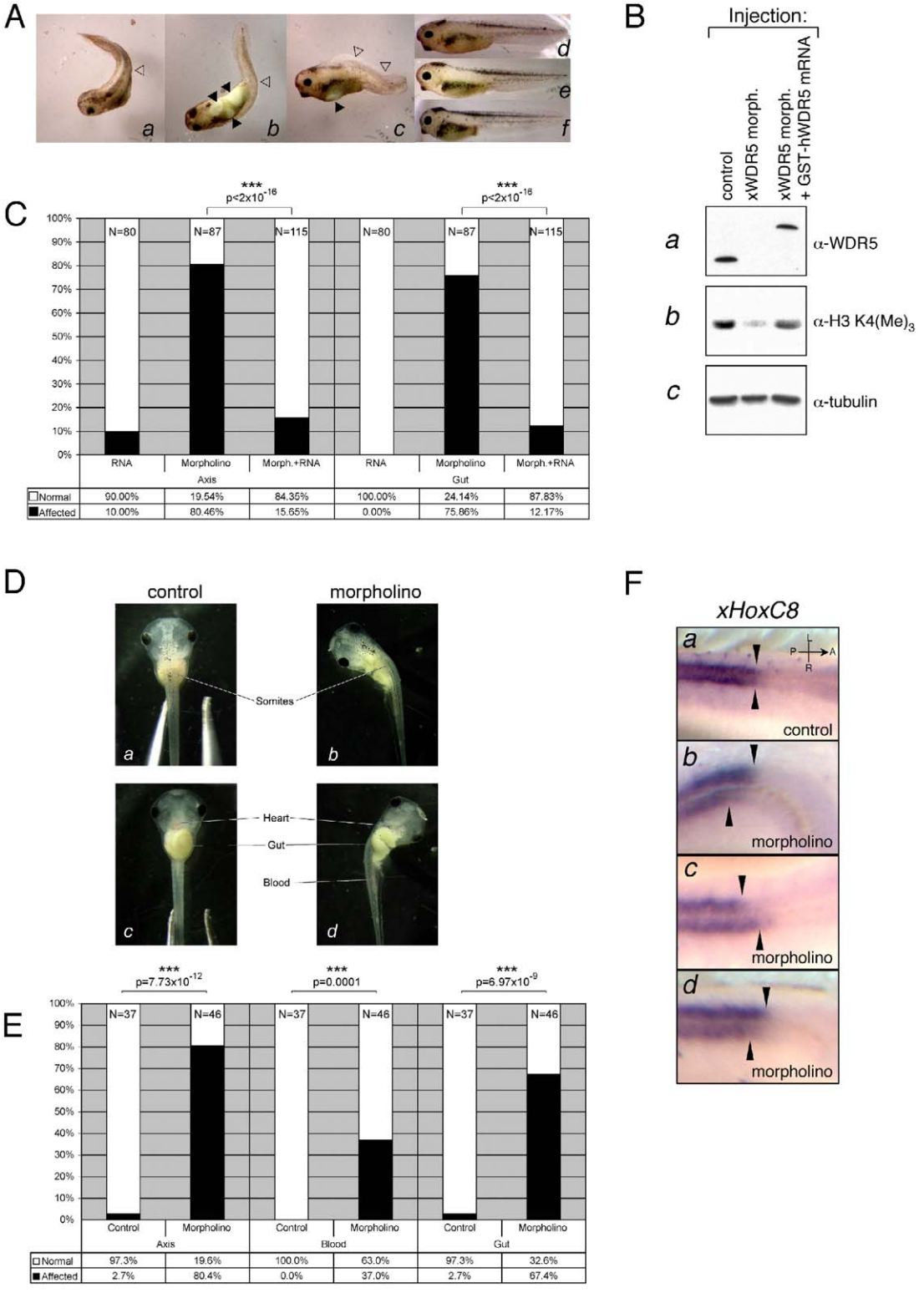

Figure 7. WDR5 Is Essential for *X. laevis* Development

(A) Dorsal (Aa), ventral (Ab), and lateral (Ac) view of stage 40 *X. laevis* tadpoles, developed from one-cell stage embryos injected with xWDR5 morpholino oligonucleotide to a final concentration of 10 μM. Axial deformities and abdominal lesions are indicated with open and closed arrowheads, respectively. Embryos coinjected with xWDR5 morpholino and GST-hWDR5 mRNA (Ad) or injected with GST-hWDR5 mRNA alone (Ae) do not significantly differ from control tadpoles (Af), indicating that phenotypes observed in (Aa)–(Ac) are the specific result of xWDR5 knockdown.

(B) Effect of xWDR5 morpholino on xWDR5 expression and H3 K4 methylation. One-cell stage embryos control injected (lane 1), injected with xWDR5 morpholino (lane 2), or coinjected with xWDR5 morpholino and GST-hWDR5 mRNA (lane 3) were developed to the tailbud stage, and

xWDR5 Knockdown Results in Abnormal Expression Pattern of *xHoxC8*

Specific somitic, hematopoetic, and gut defects observed in xWDR5-depleted tadpoles point to the abnormal regulation of the *Hox* genes. For example, HoxC8 depletion in *X. laevis* results in severe defects of abdominal structure that are reminiscent of the phenotype observed with the WDR5 knockdown (Ko and Chung, 2003). Furthermore, loss of WDR5 in human cells leads to decrease of *HOXC8* expression.

To address whether xWDR5 knockdown leads to the deregulation of *xHoxC8* expression, we used in situ hybridization to visualize *xHoxC8* spatial expression pattern in tadpoles derived from two-cell stage embryos injected with xWDR5 morpholino into one blastomere. As shown in Figure 7F, xWDR5 knockdown resulted in the misalignment of *xHoxC8* expression domain by at least one somite length (compare control panel Figure 7Fa with Figures 7Fb–7Fd). In addition, the injected side frequently exhibited diminished levels of *xHoxC8*-specific staining. Together, these results demonstrate that WDR5 is important for proper maintenance and spatial control of *Hox* gene expression during development.

Discussion

There is growing recognition of the importance of histone methylation as an epigenetic regulatory mark that mediates activation or repression of specific genomic loci or chromosomal domains. In particular, establishment and maintenance of heterochromatin have been shown to involve methylation of H3 K9, which is read by the effector protein HP1 (reviewed in Elgin and Grewal [2003]). HP1 itself, however, associates with H3 K9 methyltransferase SUV39H1 (Aagaard et al., 1999) and is a critical determinant for H3 K9 methylation spreading (Hall et al., 2002). We propose that a similar paradigm may be extended for positive regulation of gene expression, in that WDR5, a component of H3 K4 methyltransferase complexes, participates both in reading and writing the H3 K4 methylation mark (see Figure 8).

WD40 Propeller: A Module for Association with the Histone Tail

WD40-repeat proteins are involved in very diverse cellular functions in which the WD40 propeller usually mediates protein-protein interactions. They are also well represented among chromatin-associated proteins. For example, EED, a WD40-repeat protein, is an essential component of the PRC2 complex. Two other WD40-repeat proteins, RbAp46 and RbAp48, are found together in a variety of chromatin-associated complexes (for reviews, see Cao and Zhang [2004], Loyola and Almouzni [2004]). Molecular modeling of the WDR5 structure reveals that it is predicted to fold into a seven-bladed propeller containing a centrally located cavity (see Figure S2). Determining where the H3 K4 methyl peptide binds (i.e., to the side, top, or internal cavity) will require future structural studies. Despite these uncertainties, our results point to a potentially novel mode of methyl-lysine histone peptide recognition that appears to be distinct from chromodomain or chromodomain-like modules.

WDR5 as an Effector Protein

We demonstrated that WDR5 is important for binding of the methyltransferase complex to the K4-dimethylated H3 tail and for global and gene-specific K4 trimethylation. In contrast, WDR5 is not required for the association of methyltranferase complexes with chromatin or for H3 K4 dimethylation. Thus, our data support the model presented in Figure 8. We envision that H3 K4 methyltransferase complex is recruited to chromatin independently of WDR5 and that this event is most likely mediated by site-specific transcriptional activators at target loci (step 1). Our data suggest that the K4 methylation pathway can be initiated independently of WDR5, as methyltransferase complex subunit(s) distinct from WDR5 associates with unmodified H3 tail substrates. Once methylation is initiated, we propose that WDR5 endows the methyltransferase complex with

endoderm was excised to eliminate egg yolk. Embryos lacking endoderm were subsequently used for whole-cell extract preparation. Extracts were analyzed by immunoblotting with α-WDR5 (Ba), α-H3 K4(Me)$_3$ (Bb), and α-tubulin (Bc) antibodies.

(C) Quantitative analysis of axial deformities ("Axis") and abdominal lesions ("Gut") present in morpholino-injected embryos ("Morpholino"), embryos coinjected with morpholino and GST-hWDR5 mRNA ("Morph.+RNA"), or injected with GST-hWDR5 mRNA alone ("RNA"). Total number of counted embryos is indicated at the top of each column. Differences between morpholino-injected and RNA + morpholino-coinjected populations are highly statistically significant ($p < 2 \times 10^{-16}$) as determined by test for equal proportions and indicated at the top of the plot. Coinjection of GST-hWDR5 mRNA with morpholino rescues the phenotypes essentially to the penetrance observed in control sample ($p = 0.35$ for axial and $p = 0.003$ for the gut defects).

(D) Feeding stage tadpoles derived from two-cell stage embryos were control injected (Da and Dc) or injected in one of the two blastomeres with 10 nl of 0.5 mM xWDR5 morpholino (Db and Dd). Morpholino-injected tadpoles exhibit axial deformation on the injected side, abnormal distribution of blood cells (blood is absent from heart while forming a hemorrhage in the tail), and failure of gut patterning.

(E) Quantitative analysis of the penetrance of phenotypes presented in (D). Number of occurrences of axial defects ("Axis"), blood distribution abnormalities ("Blood"), and gut coiling defects ("Gut") were noted in mock injected ("Control") and morpholino injected ("Morpholino") and plotted as proportions in total population counted. Total number of counted embryos is indicated at the top of each column. Observed differences are highly statistically significant ($p \leq 0.0001$, test for equal proportions), and the p values are indicated at the top of the plot.

(F) Whole-mount in situ detection of xHoxC8 transcript. Dorsal view of midtrunk region of stage 30 tadpoles derived from embryos control injected (Fa) or injected at two-cell stage in one of the blastomeres with xWDR5 morpholino (Fb–Fd) is shown. Purple stain indicates *xHoxC8* expression, which is most prominent in neural tube. Arrows indicate misalignment of the *xHoxC8* expression domains between left and right side of neural tube in morpholino-injected but not control embryos. All images are shown in the same orientation (see [Fa], upper right corner: A–P, anterior-posterior axis; L–R, left-right axis).

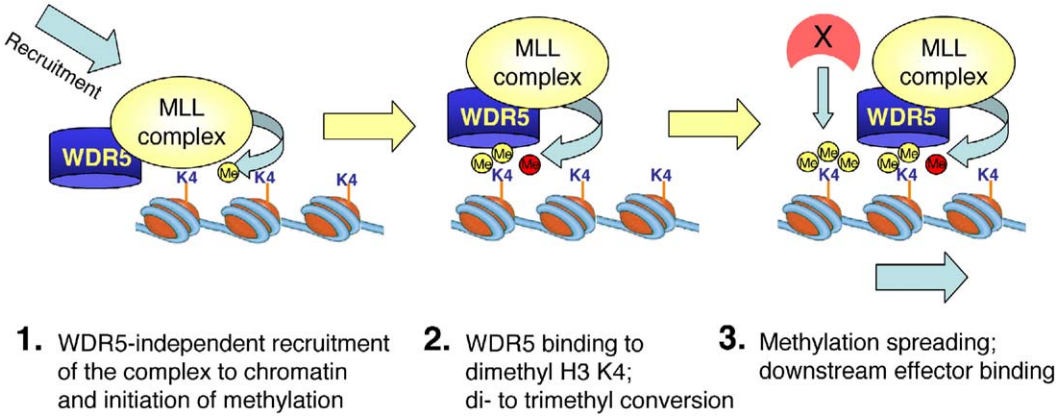

Figure 8. Model for WDR5's Role in Activation of Gene Expression

(1) H3 K4 methyltransferase complex is recruited to chromatin in a reaction dependent upon binding to unmodified H3 tails, resulting in initiation of methylation. (2) Once methylation is initiated, WDR5 endows the H3 K4 methyltransferase complex with an ability to bind to dimethylated substrates and is important for di- to trimethyl conversion at K4. (3) As the methyltransferase complex does not bind efficiently to the trimethylated tail, we propose that it is then released from its substrate, resulting in the binding to the nearby nucleosome and propagation of the methylation signal. Trimethylation may then lead to the recruitment of downstream effector proteins and activation of transcription. WDR5's role in H3 K4 monomethylation is not yet clear.

an ability to bind to dimethylated substrate and is important for di- to trimethyl conversion (step 2). Such a model is consistent with the fact that dimethylated H3 K4 peptide can be further methylated by the WDR5-containing hSet1 and MLL1 complexes (Wysocka et al., 2003; Dou et al., 2005) but not by recombinant MLL1 SET domain (Milne et al., 2002; Nakamura et al., 2002). As methyltransferase complex does not appear to bind efficiently to the trimethylated tail, we suspect that the complex is then released from its substrate, which can result in the binding to the nearby nucleosome and propagation of the methylation signal. Trimethylation may then lead to the recruitment of downstream effector proteins and activation of transcription by pathways that are still largely unknown (step 3). This proposed model is also consistent with the transactivation properties of the WDR5 protein, as trimethylation of H3 K4 is associated with promoter and 5′ transcribed regions of active genes (Santos-Rosa et al., 2002; Schneider et al., 2004).

Role of WDR5 and H3 K4 Methylation in Development and Differentiation

A WDR5 homolog, Swd3, exists in yeast *S. cerevisiae*, where it has been shown to be a component of the yeast Set1 complex (Roguev et al., 2001; Miller et al., 2001; Nagy et al., 2002). Swd3 is nonessential for viability, but is essential for the H3 K4 methylation in yeast (Miller et al., 2001; Nagy et al., 2002). In contrast, we report here that WDR5 is essential both for viability and for H3 K4 methylation in vertebrates. Furthermore, *D. melanogaster* WDR5 homolog, called "will die slowly" (wds) is encoded by an essential gene (Hollmann et al., 2002). These observations suggest that H3 K4 methylation is essential in multicellular as opposed to unicellular organisms. Steady-state levels of H3 K4 methylation are considerably higher in bulk histone preparations isolated from unicellular eukaryotes as compared to multicellular organisms, a result anticorrelated with H3 K9 methylation (Briggs et al., 2001). These data hint at the intriguing possibility that the epigenetic "default state" in multicellular organims is set more to a silencing mode. If correct, regulated gene activation, in part dictated by activating marks such as H3 K4 methylation, may play a more important role in muticellular organisms, where complex developmental processes, involving cellular differentiation, are critical. In support, WDR5 is important for maintenance of *Hox* gene expression in human cells and during *Xenopus* development. Furthermore, mesodermal and endodermal patterning defects observed in the WDR5-depleted *X. laevis* tadpoles are consistent with differentiation defects arising through abnormalities in homeotic gene expression.

In sum, our data provide evidence that WDR5 is an important regulator of gene expression by acting as a "sensor" protein that participates in both reading and writing the H3 K4 methyl mark. Perturbations in gene expression patterns caused by loss of WDR5 result in abnormal execution of developmental programs, underscoring crucial roles of the epigenetic signal of H3 K4 methylation in differentiation and development.

Experimental Procedures

Pull-Down Assays

Nuclear extracts were prepared from 293 cells using Dignam protocol (Dignam et al., 1983), precleared with avidin beads, and incubated with peptide prebound to avidin beads for 3 hr at 4°C. About 5 μg of peptide and 10^8 cells were used per pull-down. Beads were washed eight times with buffer containing 20 mM HEPES (pH 7.9), 300 mM KCl, 0.2% Triton X-100, 1 mM PMSF, and protease inhibitor cocktail (Roche). A final wash was performed with buffer containing 4 mM HEPES (pH 7.9), 10 mM NaCl, 1 mM PMSF, and protease inhibitor cocktail (Roche). Bound proteins were eluted from the resin two times with 100 mM glycine (pH 2.8). Eluates were combined, neutralized using 1/10 volume of 1 M Tris (pH 8), and analyzed by SDS PAGE. For peptide competition experiments, proteins bound to the resin were incubated with 20-fold molar excess of the competing peptide for 20 min at RT.

Chromatin Fractionation and Isolation of Mononucleosomal Fraction

The biochemical fractionation procedure and micrococcal nuclease treatment were performed as described (Wysocka et al., 2001; Mendez and Stillman, 2000). Samples that were determined to contain only mononuclesomal DNA were pooled and used for the coimmunoprecipitation assays.

Coimmunoprecipitation

Mononucleosomal fractions were prepared from a HeLa cell line stably expressing Flag/HA-tagged full-length WDR5 (Dou et al., 2005) and as a control from HeLa cells lacking ectopic WDR5. Mononucleosomal fractions were then incubated with FLAG M2 agarose beads (Sigma). Immunoprecipitates were washed and eluted from beads with Flag peptide (Sigma) at concentration of 0.5 mg/ml.

Antibodies

α-WDR5 and α-Ash2 affinity-purified rabbit polyclonal antibodies were kind gifts of W. Herr; α-MLL1 rabbit polyclonal antibody was described in Dou et al. (2005); other antibodies were obtained commercially: α-RbBP5 and α-MLL2 (Bethyl Laboratories); α-H3 K4 mono-, di-, and trimethyl (Upstate Biotechnology and Abcam); α-H3 K9 trimethyl, α-H3 K27 trimethyl, α-H3 1-20 unmodified, and α-HP1 (Upstate Biotechnology); and α-tubulin (Sigma).

Luciferase Assays

A 293T cell line stably expressing luciferase reporter under the control of tandem of five GAL4 UAS sites was transfected using Lipofectamine 2000 (Invitrogen) with indicated amounts of pCMX-GAL4 DNA binding domain (DBD) or pCMX-GAL4 full-length WDR5 expression vectors or mock transfected. In each case, pUC119 DNA was additionally added to make up for a total of 4 μg of transfected DNA. Cells were normalized by counting and then lysed, and luciferase assay kit (Promega) was used to determine relative levels of the luciferase gene product.

WDR5 Knockdown in Human Cells

Human WDR5 siRNA SMART pool consisting of four siRNA duplexes was purchased from Dharmacon. 293 cells were seeded on 6-well plates and transfected with siRNA SMART pool or each of four individual WDR5 SMART duplexes by using Lipofectamine 2000 (Invitrogen) according to the manufacturer's instructions. A corresponding amount of noncoding siRNA duplexes (Dharmacon) was used for control transfections. One additional round of transfection was performed using identical conditions 24 hr after the initial transfection. Cells were harvested 72 hr after second transfection and were either lysed in SDS Laemmli buffer, subjected to RNA preparation, or fixed with formaldehyde for ChIP analysis.

Chromatin Immunoprecipitation and Q-PCR Detection

Chromatin Immunoprecipitations (ChIPs) were performed using the Chromatin Immunoprecipitation Assay Kit (Upstate Biotechnology) and the following antibodies: histone H3 K4$(Me)_2$ (ab7766-50) and H3 K4$(Me)_3$ (ab8580-50) both from Abcam, and H3 K4$(Me)_3$ (07-473) from Upstate Biotechnology. Anti-MLL_C is described in Dou et al. (2005). Real-time PCR quantification of ChIP was performed in triplicate using Taqman probes and a Stratagene Mx3000p. ChIP was quantified relative to inputs using the method described in Frank et al. (2001).

HOX Gene Expression

Total RNA was isolated using RNeasy columns (Qiagen), treated with DNase, and reverse transcribed (SuperScript, Invitrogen). Real-time PCR quantification of *Hox* gene expression was performed in triplicate using Taqman probes and a Stratagene Mx3000p instrument using a standard curve and the relative quantitation method as described in ABI User Bulletin 2. βACTIN and *GAPDH* probes and primers used were from Applied Biosystems Inc.

In Vitro Transcription

Synthetic open reading frame encoding human GST-WDR5 fusion protein was cloned into pCS2+ vector, and 5′-capped mRNAs were transcribed in vitro from the SP6 promoter of the HpaI-linearized template using the mMessageMachine kit (Ambion).

Morpholino Design and xWDR5 Knockdown

BLAST analysis of database EST sequences provides evidence that *X. laevis* WDR5 is encoded by two distinct yet closely related genes. Morpholino oligonucleotide of the sequence 5′-CATGGTGT CAGCACTAGAATGGTGC-3′ targeting ATG region of both putative *X. laevis* WDR5 mRNAs was synthesized by Gene Tools, LLC, and handled according to manufacturer's specifications. One or two cell stage embryos were injected with 20 and 10 nl, respectively, of 1 mM morpholino solution or 1 mM morpholino with 50 ng/μl synthetic human GST-WDR5 mRNA and grown at 18°C. Embryos were transferred into 0.1 × MMR + 50 μg/ml gentamycin prior to gastrulation. Number of clear phenotypical abnormalities was noted in observed population of injected embryos. Statistical significance of the differences in phenotype frequency between experimental samples and control was determined by test for equal proportions (function prop.test in R statistical suite [R Development Core Team, 2004]).

Immunostaining of *Xenopus* Embryos

Stage 11 *Xenopus* embryos were fixed, and immunostaining was performed according to Brivanlou and Harland (1989) protocol. Prior to observation, embryos were brought to RT and cleared with 2:1 benzyl benzoate:benzyl alcohol solution, and in situ fluorescence was visualized with Zeiss Pascal LSM confocal microscope.

In Situ Hybridization

cDNA fragment corresponding to the *xHoxC8* open reading frame was amplified by PCR from *X. laevis* stage 30 cDNA and cloned into pCS2+ vector. Digitoxin-labeled riboprobe was synthesized by in vitro transcription with T7 RNA polymerase using DIG labeling mix from Roche. Staged embryos were fixed, and in situ hybridization was performed as described in Sive et al. (2000). Probe was detected with AP-conjugated anti-DIG antibodies followed by color reaction with BM Purple reagent (Roche).

Supplemental Data

Supplemental Data include two figures and can be found with this article online at http://www.cell.com/cgi/content/full/121/6/859/DC1/.

Acknowledgments

We thank W.K. Wang and D. Patel for molecular modeling of WDR5; W. Herr for α-WDR5 and α-Ash2 antibodies; M. Guenther for advice on pull-down assays; F. Spagnoli and A. Vonica for advice on *Xenopus* techniques; W. Fischle for recombinant HP1β protein; and R. Cook, C. McDonald, and RU Proteomics Resource Center for peptide synthesis. We are grateful to members of the Allis and Brivanlou labs for helpful discussions and to W. Herr, A. Vonica, S. Hake, E. Bernstein, E. Duncan, and S. Taverna for critical readings of the manuscript. J.W. is a Damon Runyon CRF fellow, T.S. is a Charles H. Revson fellow, and Y.D. is an Irvington Institute for Immunology fellow. This work was supported by NIH grants: MERIT Award (GM 53512) to C.D.A., R01 GM066977 to A.H.B., and NCRR RR015804 and RR001614 to A.L.B.

Received: January 26, 2005
Revised: March 14, 2005
Accepted: March 31, 2005
Published: June 16, 2005

References

Aagaard, L., Laible, G., Selenko, P., Schmid, M., Dorn, R., Schotta, G., Kuhfittig, S., Wolf, A., Lebersorger, A., Singh, P.B., et al. (1999). Functional mammalian homologues of the *Drosophila* PEV-modifier

Su(var)3–9 encode centromere-associated proteins which complex with the heterochromatin component M31. EMBO J. *18*, 1923–1938.

Bannister, A.J., Zegerman, P., Partridge, J.F., Miska, E.A., Thomas, J.O., Allshire, R.C., and Kouzarides, T. (2001). Selective recognition of methylated lysine 9 on histone H3 by the HP1 chromo domain. Nature *410*, 120–124.

Briggs, S.D., Bryk, M., Strahl, B.D., Cheung, W.L., Davie, J.K., Dent, S.Y., Winston, F., and Allis, C.D. (2001). Histone H3 lysine 4 methylation is mediated by Set1 and required for cell growth and rDNA silencing in *Saccharomyces cerevisiae*. Genes Dev. *15*, 3286–3295.

Brivanlou, A.H., and Harland, R.M. (1989). Expression of an engrailed-related protein is induced in the anterior neural ectoderm of early *Xenopus* embryos. Development *106*, 611–617.

Cao, R., and Zhang, Y. (2004). The functions of E(Z)/EZH2-mediated methylation of lysine 27 in histone H3. Curr. Opin. Genet. Dev. *14*, 155–164.

Dignam, J.D., Lebovitz, R.M., and Roeder, R.G. (1983). Accurate transcription initiation by RNA polymerase II in a soluble extract from isolated mammalian nuclei. Nucleic Acids Res. *11*, 1475–1489.

Dou, Y., Milne, T.A., Tackett, A.J., Smith, E.R., Fukuda, A., Wysocka, J., Allis, C.D., Chait, B.T., Hess, J.L., and Roeder, R.G. (2005). Physical association and coordinate function of the H3 K4 methyltransferase MLL1 and the H4 K16 acetyltransferase MOF. Cell *121*, this issue, 873–885.

Elgin, S.C., and Grewal, S.I. (2003). Heterochromatin: silence is golden. Curr. Biol. *13*, R895–R898.

Francis, N.J., and Kingston, R.E. (2001). Mechanisms of transcriptional memory. Nat. Rev. Mol. Cell Biol. *2*, 409–421.

Frank, S.R., Schroeder, M., Fernandez, P., Taubert, S., and Amati, B. (2001). Binding of c-Myc to chromatin mediates mitogen-induced acetylation of histone H4 and gene activation. Genes Dev. *15*, 2069–2082.

Goo, Y.H., Sohn, Y.C., Kim, D.H., Kim, S.W., Kang, M.J., Jung, D.J., Kwak, E., Barlev, N.A., Berger, S.L., Chow, V.T., et al. (2003). Activating signal cointegrator 2 belongs to a novel steady-state complex that contains a subset of trithorax group proteins. Mol. Cell. Biol. *23*, 140–149.

Hall, I.M., Shankaranarayana, G.D., Noma, K., Ayoub, N., Cohen, A., and Grewal, S.I. (2002). Establishment and maintenance of a heterochromatin domain. Science *297*, 2232–2237.

Hollmann, M., Simmerl, E., Schafer, U., and Schafer, M.A. (2002). The essential *Drosophila melanogaster* gene wds (will die slowly) codes for a WD-repeat protein with seven repeats. Mol. Genet. Genomics *268*, 425–433.

Hughes, C.M., Rozenblatt-Rosen, O., Milne, T.A., Copeland, T.D., Levine, S.S., Lee, J.C., Hayes, D.N., Shanmugam, K.S., Bhattacharjee, A., Biondi, C.A., et al. (2004). Menin associates with a trithorax family histone methyltransferase complex and with the hoxc8 locus. Mol. Cell *13*, 587–597.

Ko, C., and Chung, H.M. (2003). *Xenopus* hoxc8 during early development. Biochem. Biophys. Res. Commun. *300*, 9–15.

Lachner, M., O'Carroll, D., Rea, S., Mechtler, K., and Jenuwein, T. (2001). Methylation of histone H3 lysine 9 creates a binding site for HP1 proteins. Nature *410*, 116–120.

Loyola, A., and Almouzni, G. (2004). Histone chaperones, a supporting role in the limelight. Biochim. Biophys. Acta *1677*, 3–11.

Mendez, J., and Stillman, B. (2000). Chromatin association of human origin recognition complex, cdc6, and minichromosome maintenance proteins during the cell cycle: assembly of prereplication complexes in late mitosis. Mol. Cell. Biol. *20*, 8602–8612.

Miller, T., Krogan, N.J., Dover, J., Erdjument-Bromage, H., Tempst, P., Johnston, M., Greenblatt, J.F., and Shilatifard, A. (2001). COMPASS: a complex of proteins associated with a trithorax-related SET domain protein. Proc. Natl. Acad. Sci. USA *98*, 12902–12907.

Milne, T.A., Briggs, S.D., Brock, H.W., Martin, M.E., Gibbs, D., Allis, C.D., and Hess, J.L. (2002). MLL targets SET domain methyltransferase activity to Hox gene promoters. Mol. Cell *10*, 1107–1117.

Nagy, P.L., Griesenbeck, J., Kornberg, R.D., and Cleary, M.L. (2002). A trithorax-group complex purified from *Saccharomyces cerevisiae* is required for methylation of histone H3. Proc. Natl. Acad. Sci. USA *99*, 90–94.

Nakamura, T., Mori, T., Tada, S., Krajewski, W., Rozovskaia, T., Wassell, R., Dubois, G., Mazo, A., Croce, C.M., and Canaani, E. (2002). ALL-1 is a histone methyltransferase that assembles a supercomplex of proteins involved in transcriptional regulation. Mol. Cell *10*, 1119–1128.

Pray-Grant, M.G., Daniel, J.A., Schieltz, D., Yates, J.R., and Grant, P.A. (2005). Chd1 chromodomain links histone H3 methylation with SAGA- and SLIK-dependent acetylation. Nature *433*, 434–438.

R Development Core Team (2004). R: A Language and Environment for Statistical Computing. R Foundation for Statistical Computing (http://www.R-project.org).

Roguev, A., Schaft, D., Shevchenko, A., Pijnappel, W.W., Wilm, M., Aasland, R., and Stewart, A.F. (2001). The *Saccharomyces cerevisiae* Set1 complex includes an Ash2 homologue and methylates histone 3 lysine 4. EMBO J. *20*, 7137–7148.

Santos-Rosa, H., Schneider, R., Bannister, A.J., Sherriff, J., Bernstein, B.E., Emre, N.C.T., Schreiber, S.L., Mellor, J., and Kouzarides, T. (2002). Active genes are tri-methylated at K4 of histone H3. Nature *419*, 407–411.

Schneider, R., Bannister, A.J., Myers, F.A., Thorne, A.W., Crane-Robinson, C., and Kouzarides, T. (2004). Histone H3 lysine 4 methylation patterns in higher eukaryotic genes. Nat. Cell Biol. *6*, 73–77.

Sims, R.J., 3rd, Nishioka, K., and Reinberg, D. (2003). Histone lysine methylation: a signature for chromatin function. Trends Genet. *19*, 629–639.

Sive, H.L., Grainger, R.M., and Harland, R.M. (2000). Early Development of *Xenopus Laevis*: A Laboratory Manual (Cold Spring Harbor, NY: Cold Spring Harbor Laboratory Press).

Wysocka, J., Reilly, P.T., and Herr, W. (2001). Loss of HCF-1 chromatin association precedes temperature-induced growth arrest of tsBN67 cells. Mol. Cell. Biol. *21*, 3820–3829.

Wysocka, J., Myers, M.P., Laherty, C.D., Eisenman, R.N., and Herr, W. (2003). Human Sin3 deacetylase and trithorax-related Set1/Ash2 histone H3–K4 methyltransferase are tethered together selectively by the cell-proliferation factor HCF-1. Genes Dev. *17*, 896–911.

Yokoyama, A., Wang, Z., Wysocka, J., Sanyal, M., Aufiero, D.J., Kitabayashi, I., Herr, W., and Cleary, M.L. (2004). Leukemia proto-oncoprotein MLL forms a SET1-like histone methyltransferase complex with menin to regulate Hox gene expression. Mol. Cell. Biol. *24*, 5639–5649.